Hindawi
Mathematical Problems in Engineering
Volume 2018, Article ID 6951647, 10 pages
https://doi.org/10.1155/2018/6951647

Research Article

Topology Optimization Analysis of Separation Mechanism for the Rice Trans-Planter

Yan-li Chen,[1] **Yi Hu**,[1] **Su-Yun Li**,[2] **and Tao Shang**[3]

[1]*School of Mechanical Science and Engineering, Jilin University, Changchun 130025, China*
[2]*Research Center, Guizhou Space Appliance CO., LTD. Shanghai 200333, China*
[3]*College of Mechanical and Electrical Engineering, Jiaxing University, Jiaxing 314001, China*

Correspondence should be addressed to Su-Yun Li; lisy1409@mails.jlu.edu.cn

Received 11 April 2018; Accepted 8 July 2018; Published 30 July 2018

Academic Editor: Sebastian Heidenreich

A mechanical topology regeneration design method based on the basic chain was presented which was reducing invalid topology design workload and improving optimization design efficiency. And it is used for configuration topology research of planetary separation mechanism of rice transplanting machine to verify its feasibility and effectiveness, which mainly consists of crank-rocker-separation mechanism, mechanical frame, planet carrier, total input shaft, and seedlings folder, and moving trajectory equation of seedling folder point A for the crank-rocker-separation mechanism is obtained according to the quadrangle vector closure principle. The topological synthesis diagram for motion chain for the CRSM was analysis by means of generalized treatment method based on theoretical optimization conditions and topological regeneration path design. The 6 kinds of topology diagram satisfying the design task for motion chair with high motion pair were obtained and the implemented mechanism diagram of kinematic chair for separation mechanism was designed based on the basic chain topology design method. The results show that topology design for the CRSM is relatively simplified for basic chain structure. And theoretical analysis of motion trajectory for the CRSM is relatively the same as the experimental results in the curve trend and relative error of angular displacement is reasonable and effective through test-rig comparative analysis with motion trajectory of crank-rocker-separation mechanism.

1. Introduction

With the rapid developing of China's urbanization and the urgent need to improve the Chinese people's livelihood, the agricultural engineering machinery industry plays an important role in the development process of the China in that a large number of agricultural engineering machinery equipment were applied to improve food productions and reduce labor costs. Plants and plant parts are eaten as food and around 2,000 plant species are cultivated for food [1]. Many of these plant species have several distinct cultivars, such as rice, wheat, and grain. The rice has a larger acreage and yield than other food crops in China; however, the average annual planting area is about 2800-3200 million hectares and accounts for about 40% of the national food crops [2]. Therefore, the intelligent agricultural machinery and equipment have attracted the attention for the ministry of agriculture in China.

Ministry of agriculture established the national development planning for the next decade in 2005, where the rice production mechanization level will be increased to 45% by 2015 [3]. However, national mechanized planting average level only was 38.5% at 2015 and less than 20% of rice-mechanized cultivation in the southwest and southern double-season area in China [4]. To cope with these problems, some research institutions and manufactures within the world have paid to the development of the design theory and optimization method. For example, the reliability-based robust design optimization (RBRDO) was proposed to minimize the variation and ensure the levels of failure probability of the system [5]. The kriging-based genetic algorithm is applied to aerodynamic design problems to reduce the number of design variables by eliminating those that have small effect on the objective function [6, 7]. An algorithm based on teaching-learning-based optimization (TLBO) is presented to solve this highly nonlinear optimization problem in the

crank-rocker mechanism system [8, 9]. The shape optimization for path synthesis of crank-rocker mechanisms using a wavelet based on the neural network was proposed to provide an approximate solution of the synthesis problem [10, 11]. Optimization design for crank-rocker mechanism based on genetic algorithm was established and solved the design requirements of rocker expectation function with MATLAB genetic algorithm toolbox [12, 13]. A structure design based on topology optimization was applicable to the thermal conductive and electromagnetic field [14–16]. A systematic method for designing fully decoupled compliant mechanisms with multiple degrees of freedom by using topology optimization was presented that an optimization formulation is posed by considering both output coupling and input coupling issues to achieve fully decoupled motion [17]. a new reliability-based topology optimization framework considering spatially varying geometric uncertainties was developed and performance measure approach is adopted to tackle the reliability constraints in the reliability-based topology optimization problem [18]. A two-phase optimization algorithm is proposed to ensure the stability of the optimization process, that is, a Level Set Method with a Bounded Diffusion for Structural Topology Optimization [19]. A new treatment of the solid boundary in the LBM is described particularly for the airfoil optimization design problem and, for a given objective function, the adjoint equation and its boundary conditions are derived analytically [20]. However, the publications devoted to topology optimization approach for the modern agricultural machinery design are relatively scarce. It is noted that the agriculture machinery can be rapidly redeveloped to get accurate motion trajectory by optimizing the structure and size parameters, if the topology optimization design can be employed to the field of intelligent rice agricultural machinery and equipment. Therefore, the survival rate of seedlings will be greatly improved, and grain yield was increasing.

2. System Structure and Theoretical Analysis for the Separation Mechanism of Rice Transplanting Machine

2.1. System Components and Working Principle. Figure 1 shows a structure diagram of the separation mechanism for rice transplanting machine; it can be seen that the crank-rocker separation mechanism is as research objective because this mechanism has a relatively simple and common features and can have a great improvement in terms of topology optimization.

The working principle is that the power flow was transmitted to input shaft 2 via the total input shaft 12 and bevel gear. The power flow was divided into two parts by fixed plate of transmission wheel 3; one part was transmitted to crank-rocker mechanism though center wheel 4 and transmission shafts 6 and 7, which is constituted by connecting rod 8 and sun wheel 9. Planetary wheel 11 is cyclical oscillation affected by sun gear 9 and middle idler gear 10. It was driven by other parts where the planet carrier 5 was uniform rotation and planetary wheel 11 is circular motion around the input shaft2 with planet carrier 5 rotating. Obviously, the planting target

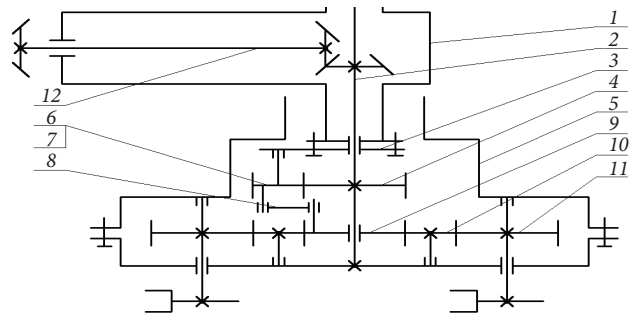

Figure 1: Configuration diagram of the planetary separation mechanism of rice transplanting machine. 1-mechanical frame; 2-input-shaft; 3-fixed plate of transmission wheel; 4-center wheel; 5-planet carrier; 6-I # transmission wheel; 7-II # transmission wheel; 8-connecting rod; 9-sun gear; 10-middle idler gear; 11-planet wheel; 12- total input shaft.

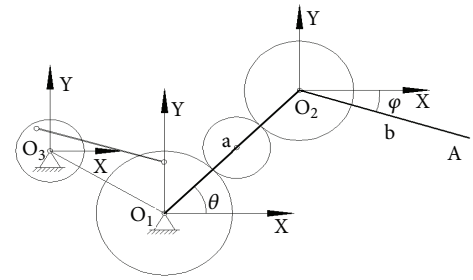

Figure 2: Simplified kinematics analysis diagram of crank-rocker separation mechanism.

trajectory of the insertion arms attached to planetary wheel 11 is the complex synthetic motion between circular motion and cyclical oscillation.

2.2. Mathematical Model. It can be seen from Figure 1 that the double insertion arms of planetary separation mechanism are symmetrically distributed and have a same law of motion when the horizontal movement of the separation mechanism is not executed. An insertion arm was used to study in order to simplify the analysis procession, and the phase angle of other insertion arm can be delayed 180 degrees [21, 22]. Obviously, if the planet carrier 5 is regarded as a lever a and the insertion arm as a lever b, the simplified kinematics analysis diagram of crank-rocker-separation mechanism (CRSM) is shown in Figure 2 and the plane motion diagram of two-bar mechanism is shown in Figure 3.

The trajectory equation of point A is obtained:

$$\begin{bmatrix} x \\ y \end{bmatrix} = \begin{bmatrix} a\cos\theta + b\cos\varphi \\ a\sin\theta + b\sin\varphi \end{bmatrix} = af(\theta) + bf(\varphi) \qquad \theta \in (\theta_1, \theta_2) \quad \varphi \in (\varphi_1, \varphi_2) \tag{1}$$

$$\theta(t) = \theta_0 + \omega t \quad t \in [0, T] \qquad \varphi(t) = \varphi_0 + \omega t \quad t \in [0, T] \tag{2}$$

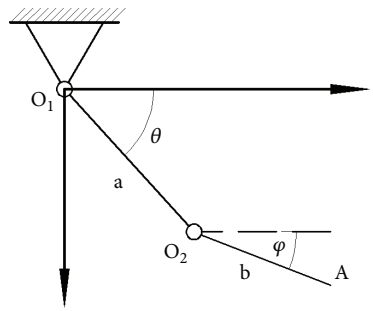

Figure 3: The plane motion diagram of two-bar mechanism.

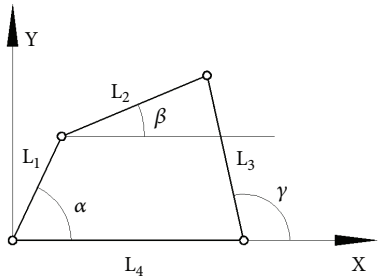

Figure 4: Kinematics analysis diagram of crank-rocker separation mechanism.

Obviously, $\theta, \varphi \in [0, 2\pi]$, a>b; the trajectory range of point A is as follows:

$$P_A \in \left[x^2 + y^2 = (a-b)^2, x^2 + y^2 = (a+b)^2\right], \quad (3)$$

where ω is angular velocity of rod A, θ is rotation angle between the rod a and x-axis, counterclockwise is positive direction, θ_0 is initial angle, φ is rotation angle between the rod b and x-axis, counterclockwise is positive direction, φ_0 is initial angle, T is the rotation period of rod a, the XO_1Y is the absolute coordinate system, the point O_1 is rotation center of planet carrier 5 for separation mechanism, the XO_2Y is the relative coordinate system on the planet carrier 5, the point O_2 is rotation center of planet wheel 11, and line O_2X is always parallel to line O_2X.

Assuming the lever joystick of crank-rocker separation mechanism is as the x-axis, the kinematics analysis diagram of crank-rocker-separation mechanism is shown in Figure 4.

According to the quadrangle vector closure principle, the following equation is obtained.

$$\overrightarrow{L_1} + \overrightarrow{L_2} = \overrightarrow{L_3} + \overrightarrow{L_4} \quad (4)$$

By substituting (1) into (4),

$$\begin{aligned} L_1 \cos(\alpha_i + \alpha_0) + L_2 \cos\beta_i &= L_4 + L_3 \cos(\gamma_i + \gamma_0) \\ L_1 \sin(\alpha_i + \alpha_0) + L_2 \sin\beta_i &= L_3 \sin(\gamma_i + \gamma_0) \end{aligned} \quad (5)$$

The rotation angle equation of link L_3 is obtained:

$$\gamma = \gamma_i + \gamma_0 = 2\arctan\frac{K_2 \pm \sqrt{K_1^2 + K_2^2 - K_3^2}}{K_1 - K_3}$$

$$\begin{aligned} K_1 &= L_4 - L_1\cos(\alpha_i + \alpha_0) \\ K_2 &= -L_1\sin(\alpha_i + \alpha_0) \\ K_3 &= \frac{\left(K_1^2 + +K_2^2 + L_3^2 - L_2^2\right)}{2L_3} \end{aligned} \quad (6)$$

According to the transmission relationship, the angle of the joystick changes the same as the angle of the lever b; that is, $\alpha_i = \omega t/2, \Delta\gamma = \Delta\phi \Longrightarrow d\gamma/dt = d\phi/dt$.

$$\varphi(t) = \varphi_0 + \frac{d\gamma}{dt}t \quad t \in [0, T] \quad (7)$$

Therefore, the trajectory equation of holding point A for the crank-rocker separation mechanism is obtained:

$$\begin{bmatrix} x \\ y \end{bmatrix} = \begin{bmatrix} a\cos(\theta_0 + \omega t) + b\cos\left(\varphi_0 + \dfrac{d\gamma}{dt}t\right) \\ a\sin(\theta_0 + \omega t) + b\sin\left(\varphi_0 + \dfrac{d\gamma}{dt}t\right) \end{bmatrix} \quad (8)$$

where L_i (i=1-4) is the length of four links for crank-rocker separation mechanism, respectively; α, β, γ is rotation angle between the link L_1, L_2, L_3 and x-axis, respectively; counterclockwise is positive direction; α_0, β_0, γ_0 is initial angle, respectively.

3. Topology Structures Analysis and Optimization Design for Planetary Distribution Mechanism of Transplanting Machine

3.1. Topological Regeneration Design Path and Processing Steps. It is all known that the mechanism topology regeneration design method is one of the famous innovative design methods and the key is that synthesis analysis of the topological structure of the kinematic chain that can reduce the workload and get an available solution.

In order to get more feasible institutions, the completely topological structure forms of kinematic chain corresponding to the initial mechanism were obtained by means theoretical analysis.

(i) For single-hinged kinematic chain on the plane, the structure formula of kinematic chain is obtained.

$$\begin{aligned} F &= 3(n-1) - 2P \\ L &= P - n + 1 \\ \sum_{i=2}^{i_{max}} n_i &= n \quad (i_{max} \le L + 1) \\ \sum_{i=2}^{i_{max}} i n_i &= 2P \quad (i_{max} \le L + 1) \end{aligned} \quad (9)$$

(ii) For kinematic chain with high-pair on the plane, the structure formula of kinematic chain is obtained.

$$F = 3(n-1) - 2P_{\text{low-pair}} - P_{high-pair}$$

$$L = P_{\text{low-pair}} + P_{high\text{-}pair} - n + 1$$

$$\sum_{i=2}^{i_{max}} n_i = n \quad (i_{max} \le L + 1) \tag{10}$$

$$\sum_{i=2}^{i_{max}} i n_i = 3(n-1) - F + P_{high-pair} \quad (i_{max} \le L + 1)$$

where F is degrees of freedom of the mechanism; N is number of components; P is the number of motion pairs in the mechanism; $P_{low-pair}$ is the number of low motion pairs in the mechanism; $P_{high-pair}$ is the number of high motion pairs in the mechanism; n_i is number of components which has i motion pair elements; L is the number of closed kinematic chains; $i_{\max}$ is the maximum number of the motion pair elements in the components.

Therefore, processing steps of topological regeneration design for topological analysis and regeneration creations were as follows [23].

Step 1. Calculate the variable parameters P and L according to the parameters n, F, and $P_{high-pair}$.

Step 2. Determining $i_{\max}$, the components number with each motion is calculated that distribution plan from n_2, n_3, …, n_{imax} is obtained, respectively.

Step 3. Neglecting the high motion pairs, a topology thumbnail on the basis of distribution plan from $n_2, n_3, \ldots, n_{imax}$ was drawn.

Step 4. The n_2 second-degree nodes are arranged to the topological thumbnails, ensuring any loops length is at least 4 and any loops length with high motion pairs is at least 3.

Step 5. Deleting stiffened and isomorphic types of mechanisms.

3.2. Generalized Treatment and Analysis. Since the axes of respective components for the separation mechanism are parallel to each other and the insertion arm portions are symmetrical, gear train diagram of separation mechanism according to the configuration diagram of separation mechanism is shown in Figure 5. It can be seen that gear train for separation mechanism is a planar kinematic chain with one degree of freedom that is composed of eight components and four high motion pairs.

Obviously, the solid dot is expressed as high motion pairs, the hollow dot is expressed as low motion pairs, and line indicates the connecting member in the motion chain diagram. The full line is expressed as high motion pairs, the broken line is expressed as low motion pairs, and dot indicates the connecting member in the topology diagram.

Admittedly, gear 2 and gear 6 are idler wheels in terms of functionality. If gear 2 and gear 6 will be ignored, this system is a planar kinematic chain with one degree of freedom that is composed of six components and two high motion pairs. Figure 6 shows simplified diagram of separation mechanism with six components and two high motion pairs.

If the simplified diagram is further processed, an abbreviated topology diagram is obtained that the points 0, 4, and 7 are removed in Figure 6(b), respectively. The Figure 7 shows the abbreviated topology diagram of separation mechanism with 6 components and 2 high motion pairs.

3.3. Topological Structure Optimization Conditions and Topological Synthesis

3.3.1. Optimization Conditions for Motion Chain. According to the theoretical analysis, the topological structure optimization conditions are as follows.

(i) The number of mechanism components is n=6; the degree of freedom F=1.

(ii) Execution component must have more than two sets of components.

(iii) The input shaft rotates at a constant speed and the actuating member should normally oscillate periodically.

(iv) There may be at least one pair of gears and speed ratio is 1:2.

(v) The topological degree of the mechanical frame is two at least and the topological degree of the original motion pieces is three at least.

3.3.2. Topological Synthesis for Motion Chain

(1) Allocation Scheme. From (10)

$$F = 3(n-1) - 2P_{\text{low-pair}} - P_{high-pair}$$

$$= 3(6-1) - 2 \times 6 - 2 = 1$$

$$L = P_{\text{low-pair}} + P_{high\text{-}pair} - n + 1$$

$$= 6 + 2 - 6 + 1 = 3$$

$$\sum_{i=2}^{i_{max}} n_i = n \Longrightarrow n_2 + n_3 + n_4 = 6 \tag{11}$$

$$\sum_{i=2}^{i_{max}} i n_i = 3(n-1) - F + P_{high-pair} \Longrightarrow$$

$$2n_2 + 3n_3 + 4n_4 = 16$$

$$i_{\max} \le L + 1 = 4$$

The allocation scheme is as follows:

Option I: $n_2 = 2, n_3 = 4, n_4 = 0$

Option II: $n_2 = 3, n_3 = 2, n_4 = 1$

Option III: $n_2 = 4, n_3 = 0, n_4 = 2$

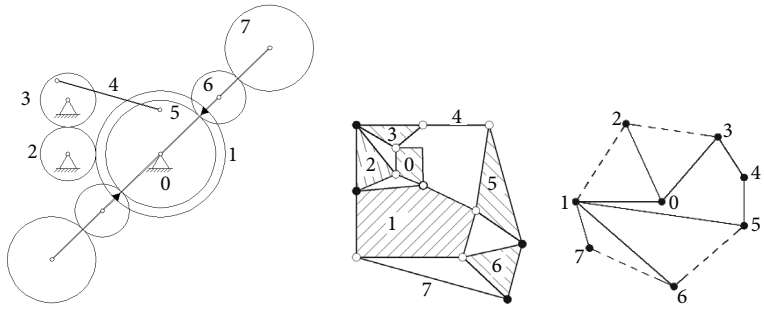

(a) Simplified component diagram (b) Motion chain diagram (c) Topology diagram

Figure 5: Diagram of gear train for separation mechanism.

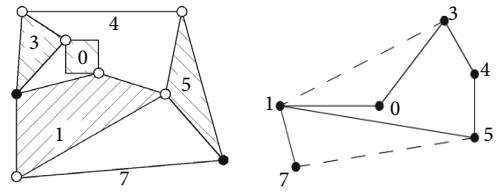

(a) Motion chain diagram (b) Topology diagram

Figure 6: Simplified diagram of separation mechanism with six components and two high motion pairs.

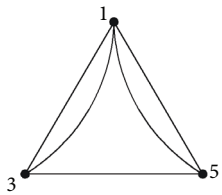

Figure 7: Abbreviated topology diagram of separation mechanism with 6 components and 2 high motion pairs.

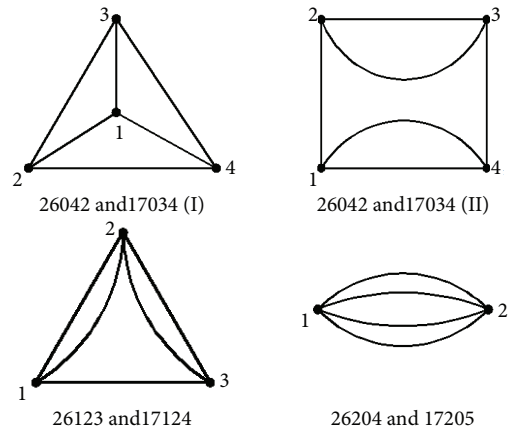

Figure 8: Abbreviated topology diagram ignored high-pair.

Since there is at least one high pair, the other high pair is replaced by one member and two rotating pairs; the allocation scheme is as follows according to (10).

Option I: $n_2 = 3, n_3 = 4, n_4 = 0$

Option II: $n_2 = 4, n_3 = 2, n_4 = 1$

Option III: $n_2 = 5, n_3 = 0, n_4 = 2$

(2) Abbreviated Topology Diagram Ignored High-Pair. The permutation order is noted as 26042, 26123, 26204,17043, 17124, and 17205 according to the number of high motion pairs, components, four members, three members, and two members [24, 25]. The abbreviated topology diagram ignored high-pair and two-degree point is shown in Figure 8.

(3) Topology Diagram within Two-Degree Point Layout. All topology diagrams within two-degree point layout are shown in Figure 9.

The topology diagram of final allocation method is shown in Figure 10, which was recorded as 26042a, 26042b, 26042c, 26123a, 26123b, and 26123c according to the optimization conditions, respectively.

Obviously, according to the design requirements, the topology design object contains high motion pair, which is to be configured. There must be a basic chain in the design mechanism, and the base chain in the separation mechanism for the rice trans-planter is shown in Figure 11.

According to the design task, the topological object is to contain the high motion pair where topological diagram of motion chain with basic chain was shown in Figure 12.

Obviously, there is redundant power transmission line after determining the basic chain for 26042c and 26123c. Removing the redundant chain, the original kinematic chain

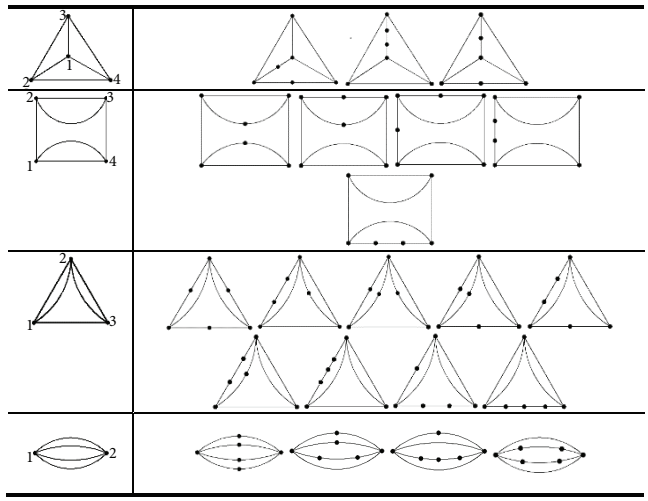

Figure 9: All topology diagrams within the two-degree point layout.

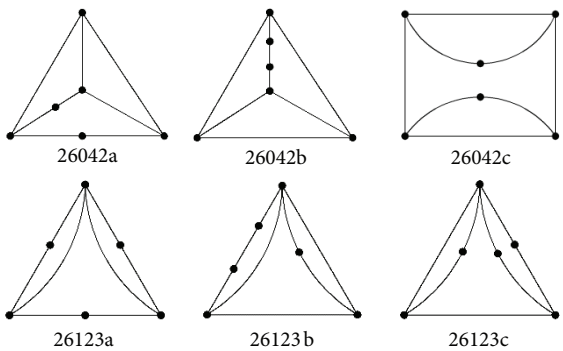

Figure 10: The topology diagram of final allocation method ignored high-pair.

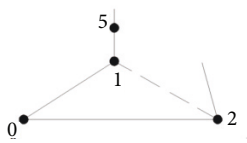

Figure 11: The topology diagram of basic chain.

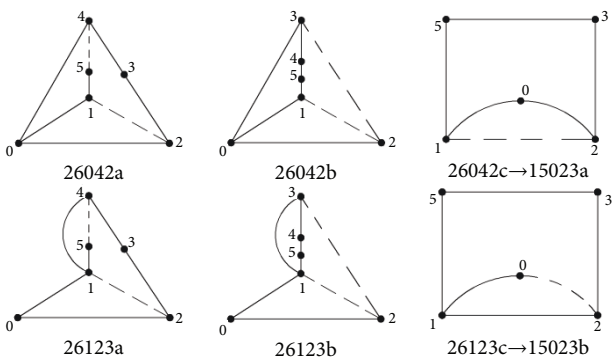

Figure 12: The topology diagram of motion chain with high motion pair.

contains 5 components and 1 high pair with 1DOF and the deformed kinematic chain is denoted by 15023a and 15023b, respectively.

3.3.3. Implementation Analysis for Motion Chain. The implemented mechanism diagram of kinematic chair for separation mechanism was shown in Figure 13 according to the working principle and optimization conditions, respectively.

4. Simulation Analysis and Example Certification for Distribution Mechanism of Transplanting Machine

4.1. Parameterized Settings and Cosimulation. From the above topology diagram, it can be seen that the other five kinds of structure have common characteristic besides the cam mechanism that member 5 is oscillated and rotated around the center of drive member 1 [26]. The simulation conditions of crank-rocker separation mechanism are shown in Table 1.

Figure 14 shows the motion trajectory of crank-rocker separation mechanism at various lengths of GC. It can be seen that the position of the inserting seeding point is almost constant horizontal coordinates with increase of length of connecting rod and the position of the removing seeding point is lower with increase of length of connecting rod.

Figure 15 shows angle curve of the CRSM under different conditions; that is, JD $\in [0, \pi]$ and GC $\in [100, 1000]$. It can be seen that the amplitude of β angular variable for member 5 is very large when the JD and GC get different values. Obviously, the maximum amplitude curves of $\beta_{\max}$ angular variable were done by using the cosimulation between Recurdyn and Matlab software which is to obtain optimization parameters according to the mechanical properties and size constraints

4.2. Bench Test. The position diagram of the inserting seeding point and the removing seeding point of bench test for the distribution mechanism are as follows.

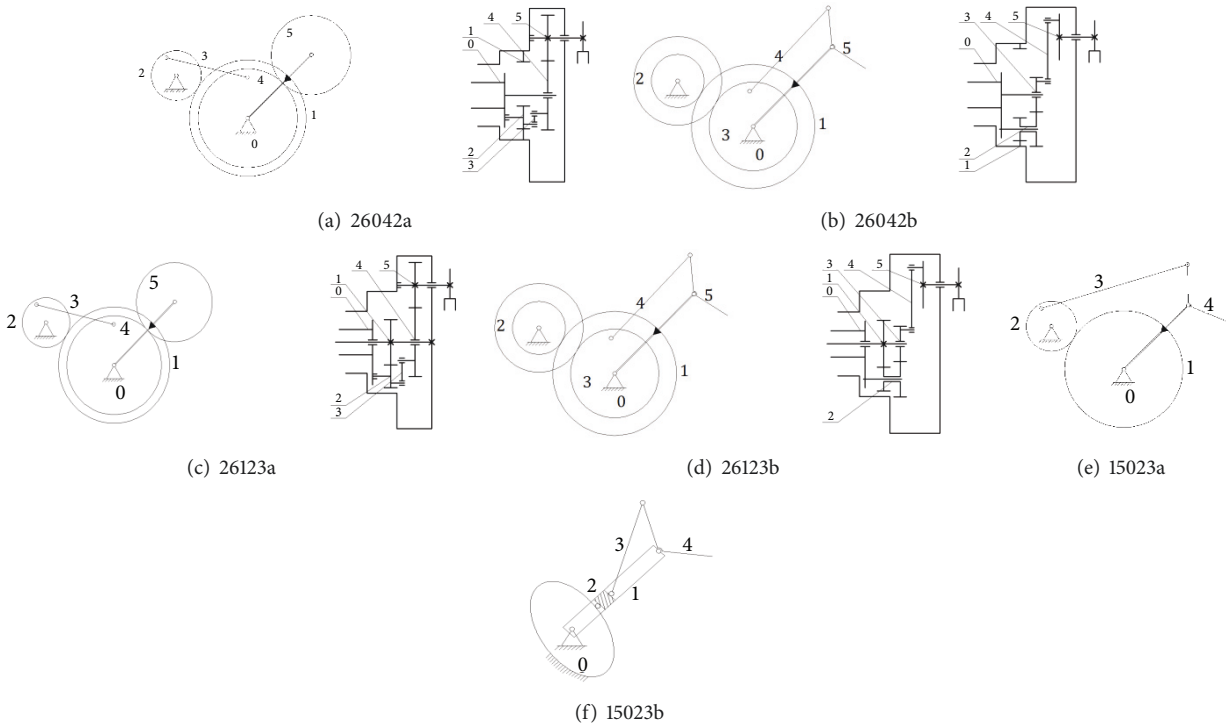

Figure 13: The implemented mechanism diagram of kinematic chair for separation mechanism.

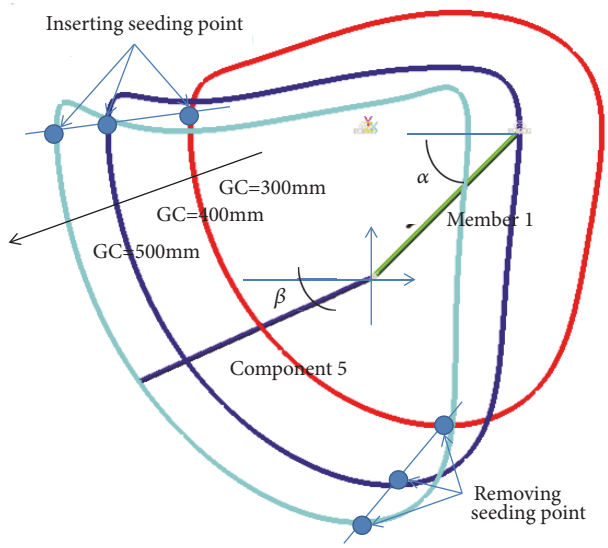

Figure 14: The motion trajectory of crank-rocker separation mechanism.

It can be seen from Figure 16 that the length LM and angle α of member 1 are 25.5mm and 5°, the length LM and angle α of member 5 are 25.5mm and 5° under the limit conditions of inserting seeding in Figure (a), respectively. Similarly, the length LM and angle α of member 1 are 28.86mm and 86° and the length LM and angle α of member 5 are 36.32mm and 19° under the limit conditions of removing seeding in Figure (b), respectively.

Obviously, the average ratio of the member 5 to the member 1 is 1.3635, the swing angle of the member 1 is 89 degrees, and the swing angle of the member 5 is 41 degrees. The length of equivalent member 1 and equivalent member 1 is 400mm and 545mm, respectively, and swing angle β of rocker member 5 is 41 degrees and the swing angle α of crank member 1 is 178 degrees according to the mathematical model of chapter 2.2. Therefore, the array of angular variables

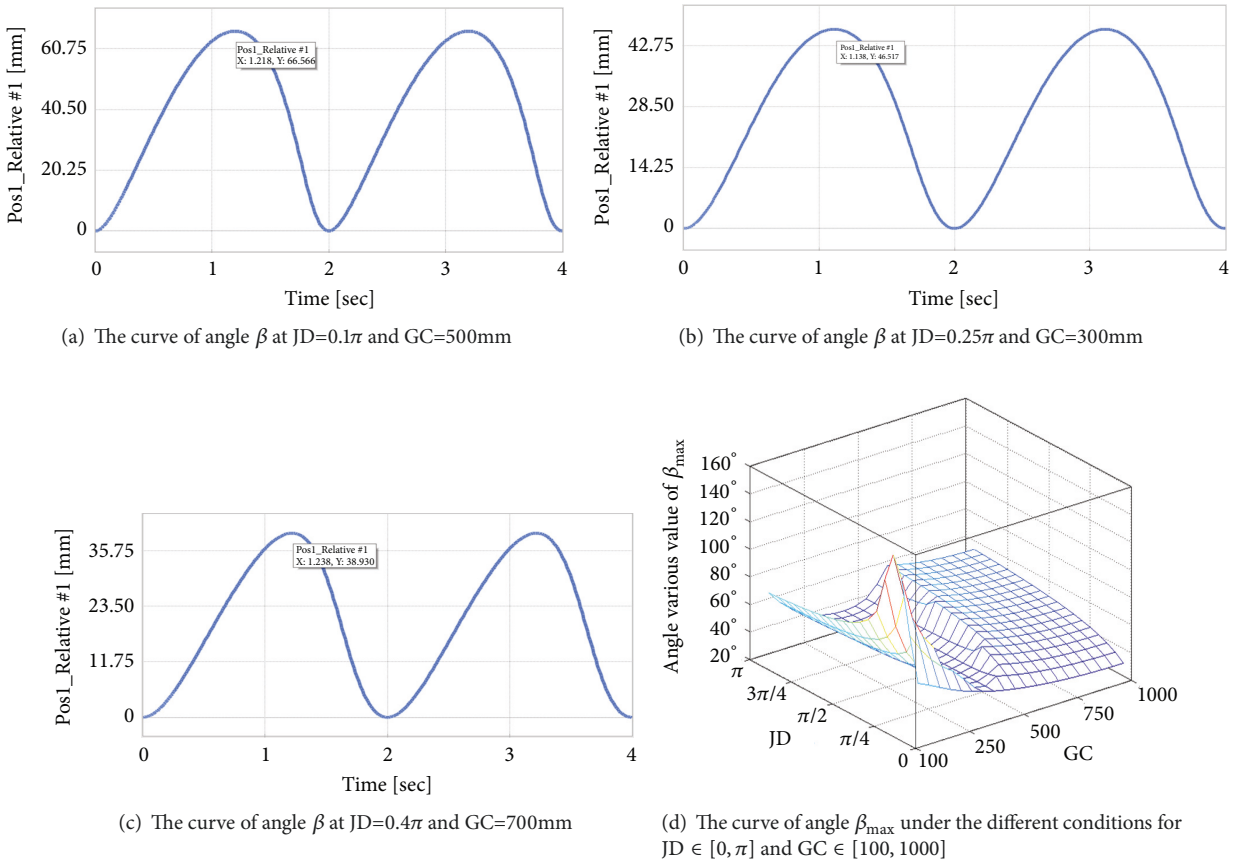

(a) The curve of angle β at JD=0.1π and GC=500mm

(b) The curve of angle β at JD=0.25π and GC=300mm

(c) The curve of angle β at JD=0.4π and GC=700mm

(d) The curve of angle β_{max} under the different conditions for JD $\in [0, \pi]$ and GC $\in [100, 1000]$

Figure 15: The angle curve of CRSM under different conditions.

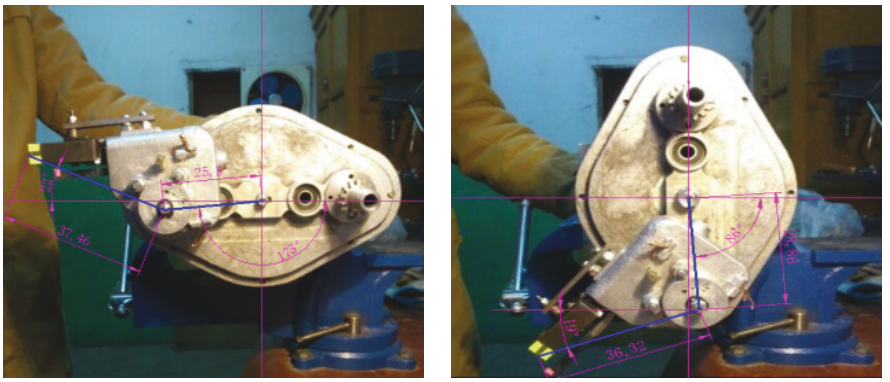

(a) (b)

Figure 16: The position diagram of the inserting seeding point and the removing seeding point for the distribution mechanism.

Z is defined to analyse the various combinations forms for JD and GC; that is, Z(JD, GC) $\in$ [39, 43]; the optimal solution is chosen among the 72 approximate solutions according to the extreme angle α of crank member 1 which is close to 178 degrees; that is, Z(JD,GC)= Z(0.3π,200). The motion trajectory of crank-rocker separation mechanism at Z(0.3π,200) is done in Figure 17. It can be seen that the theoretical analysis of motion trajectory for the CRSM is the same as the experimental results in the curve trend by contrast with Figures 16 and 17. And the extreme angle relative error is 8 degrees meeting the design requirements where angle α of crank member1 is close to 178 degrees in test and angle α of crank member 1 is 186 degrees in theory

5. Conclusions

The conclusions can be drawn as follows.

Table 1: Main parameters of the CRSM.

Name	Parameter	value
YG	Rotation center of member 1	300, 0, 0
QB	Coordinate center of the CRSM	0, 0, 0
LG1	Coordinate 1 of connecting rod	100 sin(JD), 100 cos(JD), 0
LG2	Coordinate 2 of connecting rod	(100 + GC) sin(JD), (100 + GC) cos(JD), 0
PP1	The coordinates of component 5	-600, 0, 0
JD	Initial angle of CRSM	0.25π
GC	The length of the connecting rod	300mm
LM	The length of the drive member 1	400mm
RC	Rotation center of the member 5	-100, 0, 0

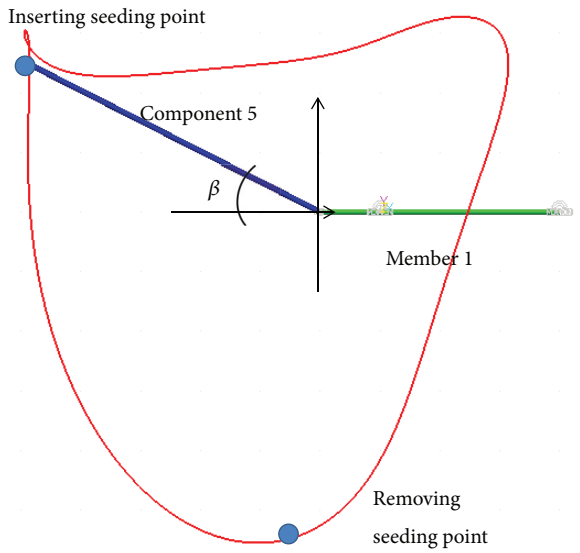

Figure 17: The Motion trajectory of CRSM at Z(0.3π,200).

(1) The system structure and working principle of separation mechanism for rice transplanter is illustrated and moving trajectory equation of holding point A for the crank-rocker separation mechanism is obtained according to the quadrangle vector closure principle.

(2) Topological regeneration design path and processing steps for theoretical optimization conditions are proposed and the topological synthesis diagram for motion chain for the CRSM was analysed by means of generalized treatment method.

(3) The 6 kinds of topology diagram satisfying the design task for motion chair with high motion pair were obtained and the implemented mechanism diagram of kinematic chair for separation mechanism was designed based on the basic chain design method.

(4) A test-rig was set up based on the working principles of the CRSM system; the results show that topology design for the CRSM is relatively simplified for basic chain structure and theoretical analysis of motion trajectory for the CRSM is the same as the experimental results in the curve trend and relative error of angular displacement is reasonable and effective through comparative analysis with motion trajectory of crank-rocker separation mechanism.

Data Availability

The data used to support the findings of this study are included within the article.

Conflicts of Interest

The authors declare that they have no conflicts of interest.

Acknowledgments

This project is supported by National Natural Science Foundation of China (Grant no. 51505174), Scientific and Technological Development Program of Jilin Province of China (Grant no. 20170101206JC), China Postdoctoral Science Foundation (Grant no. 2014M560232), Foundation of Education Bureau of Jilin Province (Grant no. JJKH20170789KJ), Research Fund for the Doctoral program of Higher Education of China (Grant no. 20130061120038), National High-Tech R&D Program of China (863 Program) (Grant no. SS2013AA060403), National key Research and development program of China (Grant no. 2017YFC0602002), and Jilin Province Key Science and Technology R&D Project (Grant no. 20180201040GX).

References

[1] Wikipedia. 2017. Food, https://en.wikipedia.org/wiki/Food#Plants.

[2] S. Xie, F. Lan, Z. M. Li, and Z. H. Su, "Curent Situation and Development Trend of Rice Transplanter at Home and Abroad," *South Agricultural Machniery*, vol. 6, pp. 38–40, 2009.

[3] China Ministry of Agriculture, 2015. National Rice Production Mechanization Decade Development Plan (2006-2015). http://www.moa.gov.cn/govpublic/NYJXHGLS/201006/t20100606_1534739.htm.

[4] W. G. Li, "Speech script on the site meeting about the whole process of rice production mechanization in china,"

http://www.amic.agri.gov.cn/nxtwebfreamwork/detail.jsp?articleId=ff8080814cfe0c72014d2c4686827a05&lanmu_id=4028800c23bb99e60123bb9d3cc2000d.

[5] M. Mayda, "An efficient simulation-based search method for reliability-based robust design optimization of mechanical components," *Mechanika*, vol. 23, no. 5, pp. 696–702, 2017.

[6] S. Jeong, M. Murayama, and K. Yamamoto, "Efficient optimization design method using kriging model," *Journal of Aircraft*, vol. 42, no. 2, pp. 413–420, 2005.

[7] Z. Zhang, L. Xu, P. Flores, and H. M. Lankarani, "A Kriging Model for Dynamics of Mechanical Systems With Revolute Joint Clearances," *Journal of Computational & Nonlinear Dynamics*, vol. 9, no. 3: 031013, 2014.

[8] R. Singh, H. Chaudhary, and A. K. Singh, "Defect-free optimal synthesis of crank-rocker linkage using nature-inspired optimization algorithms," *Mechanism and Machine Theory*, vol. 116, pp. 105–122, 2017.

[9] T. Dede, "Application of teaching-learning-based-optimization algorithm for the discrete optimization of truss structures," *KSCE Journal of Civil Engineering*, vol. 18, no. 6, pp. 1759–1767, 2014.

[10] G. Galan Marin, F. J. Alonso, and J. M. D. Castillo, "Shape optimization for path synthesis of crank-rocker mechanisms using a wavelet based on the neural network," *Mechanism Machine Theory*, vol. 44, no. 6, pp. 1132–1143, 2009.

[11] A. Smaili and N. Diab, "A new approach to shape optimization for closed path synthesis of planar mechanisms," *Journal of Mechanical Design*, vol. 129, no. 9, pp. 941–948, 2007.

[12] Z. W. Tang, Y. H. Liu et al., "Optimization Design for Crank-rocker Mechanism Based on Genetic Algorithm," in *Proceedings of the International Conference on Intelligent System design & Engineering Application*, pp. 417–420, 2012.

[13] M. Khorshidi, M. Soheilypour, M. Peyro, A. Atai, and M. Shariat Panahi, "Optimal design of four-bar mechanisms using a hybrid multi-objective GA with adaptive local search," *Mechanism and Machine Theory*, vol. 46, no. 10, pp. 1453–1465, 2011.

[14] J. H. Zhu, K. K. Yang, and W. H. Zhang, "Backbone cup – a structure design competition based on topology optimization and 3D printing," *International Journal for Simulation & Multidisciplinary Design Optimization*, vol. 7 :A1, 2016.

[15] K. Long and J. Jia, "Periodic topology optimization design for thermal conductive structure using ICM method," *Engineering Mechanics*, vol. 32, no. 5, pp. 227–235, 2015.

[16] S. Zhou, W. Li, Y. Chen, G. Sun, and Q. Li, "Topology optimization for negative permeability metamaterials using level-set algorithm," *Acta Materialia*, vol. 59, no. 7, pp. 2624–2636, 2011.

[17] B. Zhu, Q. Chen, M. Jin, and X. Zhang, "Design of fully decoupled compliant mechanisms with multiple degrees of freedom using topology optimization," *Mechanism and Machine Theory*, vol. 126, pp. 413–428, 2018.

[18] Z. Kang and P. Liu, "Reliability-based topology optimization against geometric imperfections with random threshold model," *International Journal for Numerical Methods in Engineering*, vol. 115, no. 1, pp. 99–116, 2018.

[19] B. L. Zhu, R. X. Wang, H. Li, and X. M. Zhang, "A Level Set Method With a Bounded Diffusion for Structural Topology Optimization," *Journal of Mechanical Design*, vol. 140, no. 7, article 071402, Article ID 071402, 2018.

[20] X. Li, L. Fang, and Y. Peng, "Airfoil design optimization based on lattice Boltzmann method and adjoint approach," *Applied Mathematics and Mechanics-English Edition*, vol. 39, no. 6, pp. 891–904, 2018.

[21] R. Q. Yuan, *Kinematics Analysis and Optimal Design of High-speed Rice Seedling Transplanting Mechanism*, Jilin University.2015, Changchun, 2015.

[22] C. Tian, *Study on Parameter Matching of High-Speed Rice Transplanter*, Jilin University.2013, Changchun, 2013.

[23] T. S. Mruthyunjaya, "Kinematic structure of mechanisms revisited," *Mechanism and Machine Theory*, vol. 38, no. 4, pp. 279–320, 2003.

[24] Y.-X. Wang and H.-S. Yan, "Computerized rules-based regeneration method for conceptual design of mechanisms," *Mechanism and Machine Theory*, vol. 37, no. 9, pp. 833–849, 2002.

[25] H. Ding, W. Cao, C. Cai, and A. Kecskeméthy, "Computer-aided structural synthesis of 5-DOF parallel mechanisms and the establishment of kinematic structure databases," *Mechanism and Machine Theory*, vol. 83, pp. 14–30, 2015.

[26] J. Z. Hong and Z. K. Pan, "Dynamics of flexible multibody systems with tree topologies," *Acta Mechanica Sinica*, vol. 8, no. 3, pp. 271–278, 1992.